Positive Effects of Walnut Meal Extracts on Memory Impairment of Alzheimer's Disease Mice Induced by D-Galactose

Honglin Lv
Yunnan University of Traditional Chinese Medicine
Dan Chen
Yunnan Institute of Tobacco Quality Inspection and Supervision
Chengmei Xu
Yunnan University of Traditional Chinese Medicine
Yage Ma
Yunnan University of Traditional Chinese Medicine
Jingjuan Yang
Yunnan University of Traditional Chinese Medicine
Chaoyin Chen
Yunnan Academy of Forestry and Grassland
Shenglan Zhao (zsl13330431529@126.com)
Yunnan University of Traditional Chinese Medicine

Research Article

Keywords: Walnut meal extracts (WMP), Alzheimer's disease (AD), Hippocampus, Transcriptome sequencing, Ribosomal

Posted Date: February 25th, 2021

DOI: https://doi.org/10.21203/rs.3.rs-209172/v1

Abstract

Walnut kernel was a traditional Chinese medicine, as well as a brain power boosting food. Walnut meal (WM) was prepared from walnut kernel by cold-press deoil, which was rich in polyphenols. In this study, we investigated the positive effects of walnut meal extracts on memory impairment of Alzheimer's disease (AD) mice induced by D-galactose. After 6 weeks of WMP treatment, the behavioral results showed that WMP could significantly improve the learning and memory of D-galactose Model (MOL) mice. The biochemical assay showed WMP could increase the amount of Acetylcholine (Ach) and reduce the oxidative stress and inflammation. Meanwhile, WMP improved the expression of neural stem cells, restored the number and the shape of neurons. The RNA-seq analysis revealed 284 differentially expressed genes in the hippocampus were regulated by WMP treatment, among which Gzma, Apol11b, H2-Q6 were up-regulated, while Rny1, Scgn, Col6a3 were down-regulated. Further analysis disclosed the differentially expressed genes were relevant to PI3K-Akt signaling pathway, FoxO signaling pathway, PPAR signaling pathway, neuroactive ligand-receptor interaction, cellular senescence, and particularly strongly interacted with the ribosomal family genes (Rpl35a, Rps27rt, Rpl3l, Rpl21, Rpl26). In addition, transcription factor Ep300 regulated genes of Cdkn1a, Spp1, and Tnfsf10 distinctly in the hippocampus, which were involved in inflammation and protein kinase. Transcription factor Pparg regulated genes of Angptl4, Fabp4, and Plin4, which were mainly expressed in PPAR (Peroxisome Proliferator-activated receptors) signaling pathway. This study might assist in identifying new targets to restore memory impairment in Alzheimer's disease.

Introduction

Alzheimer’s disease (AD) was the most common neurodegenerative disorder with memory, judgment, and abstract thinking disorders in the clinic[1]. With the increasing aging population around the world, AD has become a world-recognized medical problem with an incidence of more than 50 million patients[2]. The pathological features of AD usually include amyloid beta protein (Aβ) plaque deposition, hyperphosphorylation of tau protein, activation of microglia, and neurons apoptosis[3]. Recent studies have revealed the correlation between AD and the inflammation process as well as oxidative stress. Oxidative stress was the main cause of aging due to the imbalance between the production and scavenging of active nitrogen free radicals (RNS) and reactive oxygen radicals (ROS). So the reduction of cellular expression, the restrained activity of antioxidant proteins, and consequently the augment of oxidative stress would play a central role in AD. The animal model of AD illustrated that immune cells in the brain could affect neurodegenerative diseases[4]. At present, two types of chemical synthetic drugs, Cholinesterase inhibitors (ChEIS) and Memantine, have been used to treat AD. ChEIS therapeutics was based on the cholinergic hypothesis, that AD patients were usually accompanied by cholinergic system dysfunction to some degree while ChEIS was able to promote the neurotransmission of cholinergic by inhibiting the activity of ACHE. The other chemotherapeutic, memantine, could bind to an ionotropic glutamate receptor NMDAR non-competitively. The activation of NMDAR would unselectively open a cation channel with high Ca^{2+} permeability, causing continuous activation of NMDA receptors[5].

Rregrettably, the AD medicines were not only with less choices but also with unapparent effect. D-galactose injection in mice could induce memory impairment accompanied by other pathological features of AD, such as brain oxidative damage, neuroinflammation, cholinergic damage[6], and decreasing of cortical neurons and hippocampal pyramidal cells[7]; [8].

Walnut, a major nut worldwide with high nutritional value, of which the kernel was rich in oils, functional fatty acids, and phenolic compounds such as flavonoids, phenolic acids, and tannins[9]. After exctracting oil from the walnut kernel by cold pressing, walnut meal (WM) has been left as residue which has not been fully utilized. The walnut meal extracts (WMP) were rich in polyphenols, which have shown the significant activites of anti-oxidation, anti-aging, hypolipidemic, and improvement of learning and memory[10]. The polyphenol substances of WMP identified by LC/MS were including gallic acid, ellagic acid, chlorogenic acid, glansreginin A, glansreginin B, rutin, vanillic acid glucoside, cumaroylquinic acid, and digalloyl glucose[11]. The purpose of this study was to explore the therapeutic effects of WMP on memory impairment of AD mice induced by D-galactose. In addition, the RNA transcriptome was used to analyze the differentially expressed genes in the hippocampus of AD mice treated by WMP.

Materials And Methods

Preparation of extracts from Walnut meal (WMP)

The walnut meals (WM) were extracted twice for 60 minutes with 50% ethanol (1:50, W/V) under reflux, and the filtrate was concentrated by Rotary Evaporator to obtain the extracts (WMP).

Materials

Walnut meals (WM) were purchased from Yunnan Huizhiyuan Food Co. Ltd. D-galactose was purchased from USA Sigma (purity ≧ 99%). The kits of superoxide dismutase (SOD), Malondialdehyde (MDA), Acetylcholine (Ach), and Acetylcholinesterase (AchE) were purchased from Nanjing Jianchen Bioengineering Company (Nanjing, China). The Mouse Interleukin 6 (IL-6) ELISA kit was purchased from CUSABIO in China.

Animals

A total of 80 male SPF Kunming mice (two months, 18-20 g) were provided by Hunan Shrek Jingda Experimental Animal Co, Ltd. (Animal certificate number: SCXK- (Hunan) 2016-0002). The mice were placed in standard temperature (22 ± 2 °C), 60% humidity, and diurnal conditions (lights on 08:00–20:00). The animals used have free access to food and water.

After a week of adaptive feeding, the experimental mice were randomly divided into 4 groups: control group (CD, n=20), D-galactose Model group (MOL, n=20), D-galactose + walnut meal extracts group (WMP-L, 800 mg/kg/d, n=20) and D-galactose + walnut meal extracts group (WMP-H, 1600 mg/kg/d, n=20). Except for the CD group, all the other groups were subcutaneously injected with D-galactose (200

mg/kg/d) for 12 weeks, and the D-galactose was dissolved in saline, while the CD group was subcutaneously injected with 0.9% normal saline (0.1 ml/10 g) every day. The WMP-L and WMP-H groups were given walnut meal extracts by intragastric administration since the eighth week, and the CD and MOL groups were intragastric administered of the same volume of normal saline.

The experiment scheme was approved by the Experimental Animal Ethics Committee of Yunnan University of Traditional Chinese Medicine, Yunnan, China. (IACUC permit number: R-0620170043), All experiments were performed in accordance with Regulations on the Administration of Experimental Animals (3rd, 2017), Guidelines on the Ethical Treatment of Laboratory Aanimals (2006) issued by the State Science and Technology Commission of china, and Animal Research Reporting of In Vivo Experiments (ARRIVE) guidelines. Experimental programs strive to reduce animal suffering by using only the necessary number of animals to produce reliable scientific data.

The novel object recognition task

The mice were carried out in a 25 × 25 ×30cm black square box. First, the mice were put into the new object recognition device and allowed to explore freely for 5 minutes. Second, the mice were placed to the new object recognition device containing two identical objects (A + B) and allowed mice to explore freely for 5 minutes on the next day. Last, object B was replaced with a new object C in a new object recognition device, and the mice were placed to a new object recognition device to explore for 5 minutes, the exploration time of different objects (A + C) was recorded on the third day. Recognition index was used to evaluate the new object recognition ability, which was defined as the difference between exploration time of novel and familiar object, and dividing the total time spend exploring two objects in the test phase[12].

Morris Water Maze Test

Morris Water Maze test used a black round pool with water (20 ± 1 °C), a depth of 45 cm, surrounded by water maze clues, and a hidden platform at 1.0 cm underwater. The MWM was divided into four quadrants, and the hidden platform was located in the fourth quadrant. The mice were placed into the water facing the wall from one of the four quadrants (Once in each quadrant) for 4 days. If the mouse successfully reached the platform within 60 s, which was allowed to stay on the platform for 15 s, if the mouse could not find the platform within 60 s, the mouse was guided and stayed on the platform for 15 s. During the testing period, the hidden platform was removed and the mouse was placed in the pool on the wall in the quadrant opposite the platform, the track and time in each mouse in each quadrant was recorded during the 60s[13].

Determination of organ index

The mice were fasted overnight and euthanized with pentobarbital sodium (40 mg/kg) at the end of the experiment. The spleen, brain, liver, and heart were separated and washed with frozen saline and weighed these organs to calculate the organ coefficient. The organ index was defined as coefficient (mg/g) = organ weight (mg) / body weight (g)[14].

Biochemical assay

The brain tissue of mice was homogenized in order to determine the biochemical indexes. The mouse brain was homogenized, and then the homogenate centrifuged for 15 min (3500 g). The supernatant was collected to determine the biochemical indexes. The levels of SOD, MDA, Ach, AchE, and IL-6 in the brain were detected by the kit instructions.

Nissl staining

The brains of the mice were completely stripped off, then fixed with 4% paraformaldehyde, embedding in paraffin, cutting into 30 μm thick brain slices. The brains were washed twice with 1 × PBS solution with the sections stained by 0.5mL Nissl solution and incubated for 15 min at 37 ℃. Fixed the slides into 95% alcohol and dehydrated twice for 2 min each time, then put the dehydrated slides into xylene for 2 min each time[15]. The number, morphological structure, and color of Nissl bodies in the area were observed by taking pictures of 40 times the size under a microscope.

Immunohistochemistry Analysis

The brains were completely stripped out from mice, and fixed in 10% paraformaldehyde after which they were dehydrated in ethanol and embedded in paraffin. The brain slices (30μm) were cut by tissue slicer, which were stained with Nestin by immunohistochemistry, dewaxing in xylene and different concentrations of ethanol, repairing solution by repairing antigen, PBS cleaning 3 times, adding Nestin antibody and incubate overnight at 4 ℃, PBS cleaning 3 times. The brain slices were stained with DVB for 15min, distilled water was added to stop, the brain slices were added to hematoxylin liquid for staining. In each slice, three visual fields in the hippocampus were photographed at 400 × magnification. The brain slices were determined using Image-Pro Plus 6.0 and the average integral optical density (IOD) was used to evaluate the expression of Nestin in neural stem cells[16].

RNA extraction, library preparation, and sequencing

In the experiment, total RNA in the hippocampus of CD, MOL, and WMP groups were extracted with triazole reagent, the integrity and concentration of total RNA were tested by Agilent Technologies 2100 RNA Nano 6000 Assay Kit[17]. According to the manufacturer's recommendations sequencing libraries were generated using NEB Next® Ultra TM RNA Library Prep Kit for Illumina® (NEB, USA), mRNA was randomly interrupted into fragments of 200bp. The strand cDNA was synthesized by random hexamer primers and M-MuLV reverse transcriptase using mRNA as template, and second-strand cDNA synthesis, cDNA adds End Repair Mix to make its flat end, then add A tail to connect the sequencing connector at 3′. The cDNA was purified using the AMPure XP system (Beckman Coulter, Beverly, USA) to select cDNA fragments of 200~300 bp in length, the cDNA was enriched by using PCR amplification. Finally, the

library was sequenced with high throughput using Illumina HiSeq4000, and the sequencing length is 150bp[18].

Quality control of reads

Quality control of Raw Data in FASTQ format in order to obtain Clean Data that can be used for subsequent analysis, the Clean Reads was sequenced with the designated mouse genome using software for sequence alignment of the second generation (HISAT2) to obtain its location information on the reference genome[19].

Differential gene expression analysis

The feature Counts software was used to calculate the FPKM (expected number of Fragments Per Kilobase of transcript sequence per Millions base pairs sequenced) of genes expression in the hippocampus of all groups, the DESeq2 software was used to analyze the differential expression of gene (DEGs) by reading count data, genes with a |log2 (fold change)| ≥ 1 and *p*-value < 0.05 were defined as difference significance.

Bioinformatics analysis of the differential expressed genes

For visualization, the volcano map and heat map were constructed using the dnet R package. The Gene Ontology, (GO, http://www.geneontology.org/) was used to analyze the biological function of DGEs, and Kyoto Encyclopedia of Genes and Genomes (KEGG) was selected to analyze the pathway of DEGs. The STRING database was used to build a PPI network, which visual analysis was carried out by Cytoscape software.

Statistical Analysis

The GraphPad Prism 7.0 software was used for statistical analysis. Behavioral tests data were expressed as the mean ± SEM, other data expressed as the mean ± SD. The data were analyzed by One-Way ANOVA following by Duncan's post-hoc test at the significant level of 0.05.

Results

Effect of WMP on behavioral experiment of Alzheimer's disease mice induced by D-galactose

Morris water maze is mainly reflecting the spatial learning and memory ability of animals. Fig.1A illustrated the escape latency of three groups continuously shortened with the increase of training days.

The MOL mice exhibited longer latency compared with CD mice from the second day, and WMP significantly restored the escape latency in MOL mice. On the fifth day, the platform was removed to conduct a positioning cruise test. The MOL mice took much longer time to find the hidden platform and stay less time in the target quadrant (Figure.1B-C). Both parameters could be significantly improved after WMP treatment in MOL mice. The swimming records illustrated that the swimming trajectory of MOL mice in the target quadrant was less than CD mice, however, which was significantly recovered after WMP treatment (Figure.1D). In the new object experiment, the recognition index of MOL mice was significantly lower than CD mice, while treatment with WMP restored the recognition index and improved their novelty cognitive ability in MOL mice (Figure.1E).

Effect of WMP on Organ Index of Alzheimer's disease mice induced by D-galactose

At the end of the experiment, the brain index, heart index, spleen index, liver index of MOL group have significantly decreased compared with CD group. Compared with MOL group, treatment with WMP could increase the brain index, spleen index, and liver index (Table 1).

Table 1: Effect of WMP on Organ Index of Alzheimer's disease mice induced by D-galactose. Columns indicated mean ± SD. Differences were expressed by ANOVA and denoted as follows: $^{\#}p < 0.05$, $^{\#\#}p < 0.01$, $^{\#\#\#}p < 0.001$, $^{\#\#\#\#}p < 0.0001$vs. CD group; * $p < 0.05$, ** $p < 0.01$ vs. MOL group.

	CD	MOL	WMP-L	WMP-H
Spleen index	9.992±2.466	4.910±0.890$^{\#\#\#\#}$	5.186±1.339	6.899±2.462*****
Liver index	53.590±7.092	36.730±3.801$^{\#\#\#\#}$	40.850±3.229*****	43.990±1.732*******
Brain index	9.775±0.734	9.219±0.388$^{\#}$	9.497±0.356	9.788±0.752*
Heart index	5.137±0.853	4.487±0.322$^{\#}$	4.365±0.565	4.797±0.662

Effects of WMP on Ach, AchE, and IL-6 of the brain in Alzheimer's disease mice induced by D-galactose

The AchE and IL-6 levels in the brain of MOL mice were significantly increased, while the Ach level was lower ($p < 0.05$), compared with CD group (Figure. 2A-C). In contrast, treatment with WMP would decrease the AchE and IL-6 levels, and increase Ach level in the brain of MOL mice ($p < 0.05$ for all).

Effects of WMP on brain oxidative damage in Alzheimer's disease mice induced by D-galactose

Oxidative damage was closely related to Alzheimer's disease. SOD level in MOL group was significantly lower than CD group ($p < 0.05$) (Figure. 2D). In contrast, only WMP-L administration would increase SOD level in MOL mice ($p < 0.05$). MDA level significantly increased in MOL group vs. CD group ($p < 0.05$). However, treatment with WMP could decrease MDA level in the brain of MOL mice ($p < 0.05$) (Figure. 2E).

Effect of WMP on brain histopathology of Alzheimer's disease mice induced by D-galactose

As seen in Figure.3, histopathological observation showed that the Nissl corpuscles of the neurons in hippocampus DG were decreased, the color of plasma became darker, and the structure of Nissl corpuscles was abnormal in MOL mice, it's the hippocampus CA3 that the Nissl corpuscles of the neurons were partially dissolved or disappeared, and the number of neurons significantly decreased. However, WMP treatment could increase the number of Nissl bodies in hippocampus (CA3, DG) neurons, the hippocampus (CA3, DG) neurons were orderly arranged with a significant increase neuron cell number.

Effect of WMP on Hippocampus Neural Stem cells of Alzheimer's disease mice induced by D-galactose

It has been found that neurodegenerative disease is caused by neuronal degeneration, senescence, loss, and death of neurons. NScS (senescence of neural stem cells) is an important factor of neurodegenerative disease, while Nestin is a classic NSCS marker. Figure.4 illustrated that the expression of Nestin in the hippocampus (CA3, DG) of MOL mice significantly decreased ($p < 0.001$). However, the expression of Nestin in hippocampus (CA3, DG) neurons of MOL mice were increased after WMP treatment, indicating that WMP treatment could promote the proliferation of hippocampus neural stem cell.

Effect of WMP on Hippocampus Neural Stem cells of Alzheimer's disease mice induced by D-galactose

It has been found that neurodegenerative disease is caused by neuronal degeneration, senescence, loss, and death of neurons. NScS (senescence of neural stem cells) is an important factor of neurodegenerative disease, while Nestin is a classic NSCS marker. Figure.4 illustrated that the expression of Nestin in the hippocampus (CA3, DG) of MOL mice significantly decreased ($p < 0.001$). However, the expression of Nestin in hippocampus (CA3, DG) neurons of MOL mice were increased after WMP

treatment, indicating that WMP treatment could promote the proliferation of hippocampus neural stem cell.

Effect of WMP on DEGs in the hippocampus of Alzheimer's disease mice induced by D-galactose

The cDNA libraries from CD, MOL, and WMP (n = 3) hippocampus of the brain were prepared and sequenced. The good quality of RNA with favorable purity was used to build the sequencing library. The quality control results showed that RNA bands were clear and no other impurities were contaminated, OD260/280 ≥ 1.9, OD260/230 ≥ 1.9, RIN ≥ 8.6. Through RNA sequencing, we achieved RNA sequencing throughput of more than 5.71GB in each hippocampus sample, and 90% of Unique reads aligned to the reference genome (Table 2).

Furthermore, to eliminate individual-specific transformation, the hippocampus from three mice in the same group were used. Venn diagram analysis showed the uniquely expressed genes and commonly expressed in CD, MOL and, WMP groups, the number of commonly expressed genes among the CD, MOL, and WMP groups were 19888, of which 594 genes were expressed in the CD and MOL groups and 115 genes were expressed in the WMP and MOL groups (Figure 5A). The differential expressed genes (DEGs) were defined as those with |log2(fold change)| ≥1 and $p < 0.05$, the DEGs were further analyzed by constructing volcanic maps. The red dots correspond to significantly up-regulated transcripts ($p < 0.05$); the green dots correspond to significantly down-regulated transcripts ($p < 0.05$); and the gray dots correspond to no stat. Figure 5B instructed that 633 genes were differentially expressed in the hippocampus of MOL group relative to CD group, where 264 were up-regulated and 369 were down-regulated. Compared with MOL group, treatment with WMP could regulate 284 differentially expressed genes, where 126 were up-regulated and 158 down-regulated (Figure 5C). In addition, cluster analysis using Euclidean distance and a hierarchical algorithm was used to show the differentially expressed genes of CD, MOL, and WMP groups. The clustering analysis showed that there was a similarity of gene expression between CD, and WMP groups. However, the gene expression of MOL group was different from CD and WMP groups (Figure. 5D). What's interesting was that compared with the CD group, 15 genes in the hippocampus of MOL mice were up-regulated, however, which were down-regulation after the WMP treatment. In addition, 20 genes of the hippocampus in MOL mice were down-regulated compared with the CD group, which were up-regulated after the WMP treatment. It is suggested that WMP treat memory impairment mainly by altering the hippocampus with these genes, which include H2-Q6 (4.35), H2-Q7 (3.44), H2-Q4 (2.17), Gzma (30.28), Pth2r (3.20), Npbwr1 (2.45), Col6a3 (0.35), Tnfsf10 (2.01), Cyp3a13 (0.46), Nanp (3.32), Rps27rt (4.33), Apol11b (8.99), Barx2 (2.56), Nxph4 (2.99), Scgn (0.30), Rny1 (0.08), and so on.

Table 2: Comparison of CD, MOL, and WMP cDNA library with the reference genome

Sample name	Total reads	Total mapped	Unique mapped
T-CD-1	52457516	50198445(95.69%)	47577061(90.70%)
T-CD-2	44929152	42981262(95.66%)	40929083(91.10%)
T-CD-3	50560398	48156331(95.25%)	45718057(90.42%)
T-MOL-1	43562928	41559866(95.40%)	39809885(91.38%)
T-MOL-2	54724000	52147214(95.29%)	49714687(90.85%)
T-MOL-3	50294482	48360406(96.15%)	45924448(91.31%)
T-WMP-1	45559774	43571375(95.64%)	41458266(91.00%)
T-WMP-2	41037328	39208853(95.54%)	37296676(90.88%)
T-WMP-3	44848818	42829451(95.50%)	40707412(90.77%)

Bioinformatics analysis of DEGs in the hippocampus of AD mice induced by D-galactose

To investigate the GO functional of the DEGs, we performed a functional classification according to Gene Ontology terms (Figure. 6A), the primary biological processes in the hippocampus affected by WMP included response to light stimulus, positive regulation of response to cytokine stimulus, hypoxanthine oxidation, positive regulation of signal transduction and inflammatory response. The most affected cellular component in the hippocampus were extracellular space, extracellular region. The molecular function associated in the hippocampus with WMP treatment were TAP binding, antigen binding, amide binding. KEGG analysis provided a platform for the systematic analysis of gene function in the networks of gene products. The main significant pathways in the hippocampus affected by WMP were related to immune, inflammatory and nerve, including ribosome, antigen processing and presentation, PPAR signaling pathway, tyrosine metabolism, cellular senescence, FoxO signaling pathway, linoleic acid metabolism, and so on (Figure. 6B). To further analyze the relationships among the DEGs [$|\log2(\text{fold change})| \geq 1$ and $p < 0.05$] in the hippocampus affected by treatment with WMP, PPI was performed using STRING database and interpreted with Cytoscape 3.6.0 (Figure. 7A). The blue circles correspond to significantly up-regulated genes by treatment with WMP, pink circles correspond to significantly down-regulated genes by WMP, and the size of the circle represents the multiple to be adjusted. In the hippocampus, 86 differentially expressed genes were connected with each other, the top 10 genes that were highly connected to other genes in PPI including Srp54a, Rpl3l, Rpl21, Rpl26, Gm10320, Gm7536M, Rpl30, Rpl35a, Rps27rt, Sec61g, which mainly existed in the ribosomal family. Ribosomal family genes (Rpl35a, Rps27rt, Rpl3l, Rpl21, Rpl26) were remarkably adjusted after administration of WMP (Fig. 7B). Further analyses of the transcription factors of these genes showed Cdkn1a, Spp1, Tnfsf10 were obviously regulated by upstream transcription factor Ep300 (Fig. 7C), which were mainly present at the PI3K-Akt signaling pathway and FoxO signaling pathway. In addition, the genes of Angptl4, Fabp4, Plin4

were obviously regulated by upstream transcription factor Pparg (Figure. 7D), which were mainly present at the PPAR signaling pathway.

Discussion

This study has explored the therapeutic effect of WMP on memory impairment in AD mice and analyzed changes of gene expression in the hippocampus. Behavioral experiment illustreated that WMP could significantly improve the memory impairment of MOL mice, boosting spatial learning, memory, and recognition abilities. Hernandez-Rabaza et al. found apoptosis of hippocampus neurons was an important reason for the decline of learning and memory ability[20]. Slice analyses of hippocampus stained with Nestin (a marker of neural stem cells) showed the number of neurons were significantly decreased, which could be improved by WMP. Neural stem cells regulated nervous system homeostasis through self-renewal and multi-directional differentiation[21]. The hippocampus played an essential role in the process of learning and memory[22]. Since the neural stem cells in which could produce new neurons and glial cells to maintain the function of the hippocampus[23]. Previous studies had reported inflammation and oxidative stress were crucial risk factors for Alzheimer's disease, and the inflammatory factor occurred in pathologically vulnerable regions of AD[24]. Our results revealed an imbalanced brain redox in MOL mice, as well as the decreased oxidoreductase forming lipid peroxide (MDA) and activated inflammation factor (IL-6). Hence, WMP displayed a powerful ability to reduce oxidative stress and anti-inflammation.

The hippocampus was a critical brain area for learning and memory in mammals, which took charge of short-term memories in daily life and specific types of memories including episodic memory and spatial memory[25]; [26]. In addition, the long-term enhancement (LTP) of the hippocampus has been recognized as the biological basis at the cell level of learning and memory activities[27]. Until now, this has been the first study to uncover the changes of genes in the hippocampus under the influence of WMP treatment in AD mice induced by D-galactose. Results have shown that WMP treatment regulated genes relevant to ribosomal, PI3K-Akt signaling pathway, FoxO signaling pathway, PPAR signaling pathway, neuroactive ligand-receptor interaction, and cellular senescence.

Ribosome played an important role in the process of protein translation and extension. The suspension of ribosomal would induce neuron apoptosis[28]; [29], and the translation level of new proteins was crucial for the learning and memory processing of neurons[30]. Ribosome transcription had priority in all cell transcription processes to adapt to ribosome production and protein synthesis, which was necessary to maintain long-term synaptic plasticity in the central nervous system[31]. Obvious ribosomal defects appeared in the Tua pathological area. The translation reduction caused by ribosome dysfunction has been considered as part of the AD process[32]. Our results showed WMP significantly regulated the ribosomal family genes (Rpl35a, Rps27rt, Rpl3l, Rpl21, Rpl26), and which genes strongly interacted.

Ribosomal family genes were the most promising targets, which involved in the rate controlling step of protein synthesis in the hippocampus. The experiment results found upstream transcription factor Ep300 obviously regulated genes of Cdkn1a, Spp1, Tnfsf10 in the hippocampus, which involved in inflammation and protein kinase. Upstream transcription factor Ep300 was a protein of aging-associated downregulation[33], of which the suppression led to an increased expression of miR-142, as well as the accumulation of peroxisomes and ROS. MiR-142 was highly expressed in Alzheimer's disease, however, Ep300 would be able to inhibit the expression level of miR-142[34-36], which named Ep300 as an attractive target for AD therapeutic. Moreover, this study also revealed the remarkable regulated ability of the upstream transcription factor Pparg to genes of Angptl4, Fabp4, Plin4, which were mainly presented at PPAR (Peroxisome proliferator-activated receptors) signaling pathway. PPARγ were found to be able to restore the neural networks by stimulating the physiological Aβ clearance mechanism[37]. Angptl4 contributed to pathological vascular remodeling in capillary CAA, which could prevent the progression of Alzheimer's disease[38]. However, it is first reported that Lipid metabolism related genes Fabp4 and Plin4 were closely related to Alzheimer's disease.

Declarations

Data availability

The dataset generated and analyzed during the current study is available from the corresponding author on reasonable request.

Author contributions

HL, DC, SZ designed the experiment, HL, DC, YM, GY and CX participated in the experimental study. HL analyzed the data and wrote the manuscript, DC, CC and SZ revised the manuscript. All authors contributed to the article and approved the submitted version.

Conflicts of interest

The authors declare that there are no conflicts of interest regarding the publication of this paper.

Funding

The present study was supported by the National Natural Science Foundation of China (Grant No. 81760735; 21466037), Yunnan Biomed Major Project (2018ZF013), Yunnan Sci & Tech Dept-YUTCM Joint Major Project (2019FF002-006), Project of Yunnan Education Department (2020Y0223), and Yunnan Province Biomedicine Major Project (202002AA100005).

References

1. Sun, M. K. Potential Therapeutics for Vascular Cognitive Impairment and Dementia. *Curr. Neuropharmacol.* **16**, 1036-1044 (2018).
2. Scopa, C. et al. Impaired Adult Neurogenesis is an Early Event in Alzheimer's Disease Neurodegeneration, Mediated by Intracellular Abeta Oligomers. *Cell Death Differ.* **27**, 934-948 (2020).
3. Wright, A. L. et al. Neuroinflammation and Neuronal Loss Precede Aβ Plaque Deposition in the hAPP-J20 Mouse Model of Alzheimer's Disease. PLoS One. **8(4)**, e59586- (2013).
4. Britschgi, M. & Wyss-Coray, T. Systemic and Acquired Immune Responses in Alzheimer's Disease. *Int. Rev. Neurobiol.* **82**, 205-233 (2007).
5. Uddin, M. S. et al. Multi-Target Drug Candidates for Multifactorial Alzheimer's Disease: AChE and NMDAR as Molecular Targets. *Mol. Neurobiol.* **58**, 281–303 (2020).
6. Turgut, N. H. et al. Effect of Capparis Spinosa L. On Cognitive Impairment Induced by D-galactose in Mice Via Inhibition of Oxidative Stress. *Turk. J. Med. Sci.* **45**, 1127-1136 (2015).
7. Sun, K., Yang, P., Zhao, R., Bai, Y. & Guo, Z. Matrine Attenuates D-Galactose-Induced Aging-Related Behavior in Mice via Inhibition of Cellular Senescence and Oxidative Stress. *Oxid. Med. Cell. Longev.* **2018**, 7108604 (2018).
8. Zhang, Q., Li, X., Cui, X. & Zuo, P. D-Galactose Injured Neurogenesis in the Hippocampus of Adult Mice. *Neurol. Res.* **27**, 552-556 (2005).
9. Chen, P., Chen, F. & Zhou, B. Antioxidative, Anti-Inflammatory and Anti-Apoptotic Effects of Ellagic Acid in Liver and Brain of Rats Treated by D-galactose. *Sci Rep*. **8**, 1465 (2018).
10. Li, Y. et al. Glycolipid Metabolism and Liver Transcriptomic Analysis of the Therapeutic Effects of Pressed Degreased Walnut Meal Extracts On Type 2 Diabetes Mellitus Rats. *Food Funct.* **11**, 5538-5552 (2020).
11. Luo, Y. et al. Optimization of Simultaneous Microwave/Ultrasonic-Assisted Extraction of Phenolic Compounds From Walnut Flour Using Response Surface Methodology. *Pharm. Biol.* **55**, 1999-2004 (2017).
12. Lian, W. et al. Multi-Protection of DL0410 in Ameliorating Cognitive Defects in D-Galactose Induced Aging Mice. *Front. Aging Neurosci.* **9**, 409 (2017).
13. Weitzner, D. S., Engler-Chiurazzi, E. B., Kotilinek, L. A., Ashe, K. H. & Reed, M. N. Morris Water Maze Test: Optimization for Mouse Strain and Testing Environment. *J Vis Exp*. e52706 (2015).
14. Liu, J. et al. Protective Effect of Walnut On D-Galactose-Induced Aging Mouse Model. *Food Sci Nutr*. **7**, 969-976 (2019).
15. Shipley, M. T., Ennis, M. & Behbehani, M. M. Acetylcholinesterase and Nissl Staining in the Same Histological Section. *Brain Res.* **504**, 353 (1990).
16. Requejo, C. et al. Changes in Day/Night Activity in the 6-OHDA-Induced Experimental Model of Parkinson's Disease: Exploring Prodromal Biomarkers. *Front Neurosci*. **14**, 590029 (2020).
17. Li, J. et al. Transcriptional Profiling Reveals the Regulatory Role of CXCL8 in Promoting Colorectal Cancer. *Front Genet*. **10**, 1360 (2019).

18. Chi, W., Gao, Y., Hu, Q., Guo, W. & Li, D. Genome-Wide Analysis of Brain and Gonad Transcripts Reveals Changes of Key Sex Reversal-Related Genes Expression and Signaling Pathways in Three Stages of Monopterus Albus. *PLoS One*. **12**, e173974 (2017).
19. Poluan, R. H. et al. Transcriptome Related to Avoiding Immune Destruction in Nasopharyngeal Cancer in Indonesian Patients Using Next-Generation Sequencing. *Asian Pac J Cancer Prev*. **21**, 2593-2601 (2020).
20. Hernández-Rabaza, V., Llorens-Martin, M. V., Velázquez-Sánchez, C., Ferragud, A. & Canales, J. J. Inhibition of Adult Hippocampal Neurogenesis Disrupts Contextual Learning but Spares Spatial Working Memory, Long-Term Conditional Rule Retention and Spatial Reversal. *Neuroence*. **159**, 59-68 (2009).
21. Le Belle Janel E et al. Proliferative Neural Stem Cells Have High Endogenous ROS Levels that Regulate Self-Renewal and Neurogenesis in a PI3K/Akt-dependant Manner. *Cell Stem Cell*. **8(1)**,59-71 (2011).
22. Dusek, J. A. & Eichenbaum, H. The Hippocampus and Memory for Orderly Stimulusrelations. *Proceedings of the National Academy of ences of the United States of America*. **94**, 7109-7114 (1997).
23. Munoz, J. R., Stoutenger, B. R., Robinson, A. P., Spees, J. L. & Prockop, D. J. Human Stem/Progenitor Cells From Bone Marrow Promote Neurogenesis of Endogenous Neural Stem Cells in the Hippocampus of Mice. *Proc Natl Acad Sci U S A*. **102**, 18171-18176 (2005).
24. Bona, D. et al. Immune-Inflammatory Responses and Oxidative Stress in Alzheimer's Disease: Therapeutic Implications. *Curr. Pharm. Design*. **16**, 6 (2010).
25. Epp, J. R., Spritzer, M. D. & Galea, L. A. Hippocampus-Dependent Learning Promotes Survival of New Neurons in the Dentate Gyrus at a Specific Time During Cell Maturation. *Neuroscience*. **149**, 273-285 (2007).
26. Kempermann, G., Kuhn, H. G. & Gage, F. H. More Hippocampal Neurons in Adult Mice Living in an Enriched Environment. *Nature*. **386**, 493-495 (1997).
27. Bliss, T. V. P. & Collingridge, G. L. A Synaptic Model of Memory: Long-Term Potentiation in the Hippocampus. *Nature*. **361**, 31-39 (1993).
28. Becker, T. et al. Structural Basis of Highly Conserved Ribosome Recycling in Eukaryotes and Archaea. *Nature*. **482**, 501-506 (2012).
29. Darnell, A. M., Subramaniam, A. R. & O'Shea, E. K. Translational Control through Differential Ribosome Pausing during Amino Acid Limitation in Mammalian Cells. *Mol. Cell*. **71**, 229-243 (2018).
30. Terrey, M. et al. GTPBP1 Resolves Paused Ribosomes to Maintain Neuronal Homeostasis. *ELife*. **9**, (2020).
31. Allen, K. D. et al. Nucleolar Integrity is Required for the Maintenance of Long-Term Synaptic Plasticity. *PLoS One*. **9**, e104364 (2014).
32. Meier, S. et al. Pathological Tau Promotes Neuronal Damage by Impairing Ribosomal Function and Decreasing Protein Synthesis. *J. Neurosci.* **36**, 1001-1007 (2016).

33. Li, Q., Xiao, H. & Isobe, K. Histone Acetyltransferase Activities of cAMP-regulated Enhancer-Binding Protein and P300 in Tissues of Fetal, Young, and Old Mice. *J Gerontol A Biol Sci Med Sci*. **57**, B93-B98 (2002).
34. Houri, K. et al. MiR-142 Induces Accumulation of Reactive Oxygen Species (ROS) by Inhibiting Pexophagy in Aged Bone Marrow Mesenchymal Stem Cells. *Sci Rep*. **10**, 3735 (2020).
35. Song, J. & Kim, Y. K. Identification of the Role of miR-142-5p in Alzheimer's Disease by Comparative Bioinformatics and Cellular Analysis. *Front Mol Neurosci*. **10**, 227 (2017).
36. Sharma, S. et al. Repression of miR-142 by P300 and MAPK is Required for Survival Signalling Via Gp130 During Adaptive Hypertrophy. *EMBO Mol. Med.* **4**, 617-632 (2012).
37. Kitagishi, Y. & Matsuda, S. Diets Involved in PPAR and PI3K/AKT/PTEN Pathway May Contribute to Neuroprotection in a Traumatic Brain Injury. *Alzheimers Res. Ther.* **5**, 42 (2013).
38. Chakraborty, A. et al. Angiopoietin Like-4 as a Novel Vascular Mediator in Capillary Cerebral Amyloid Angiopathy. *Brain : a journal of neurology*. **141**, 3377-3388 (2018).

Figures

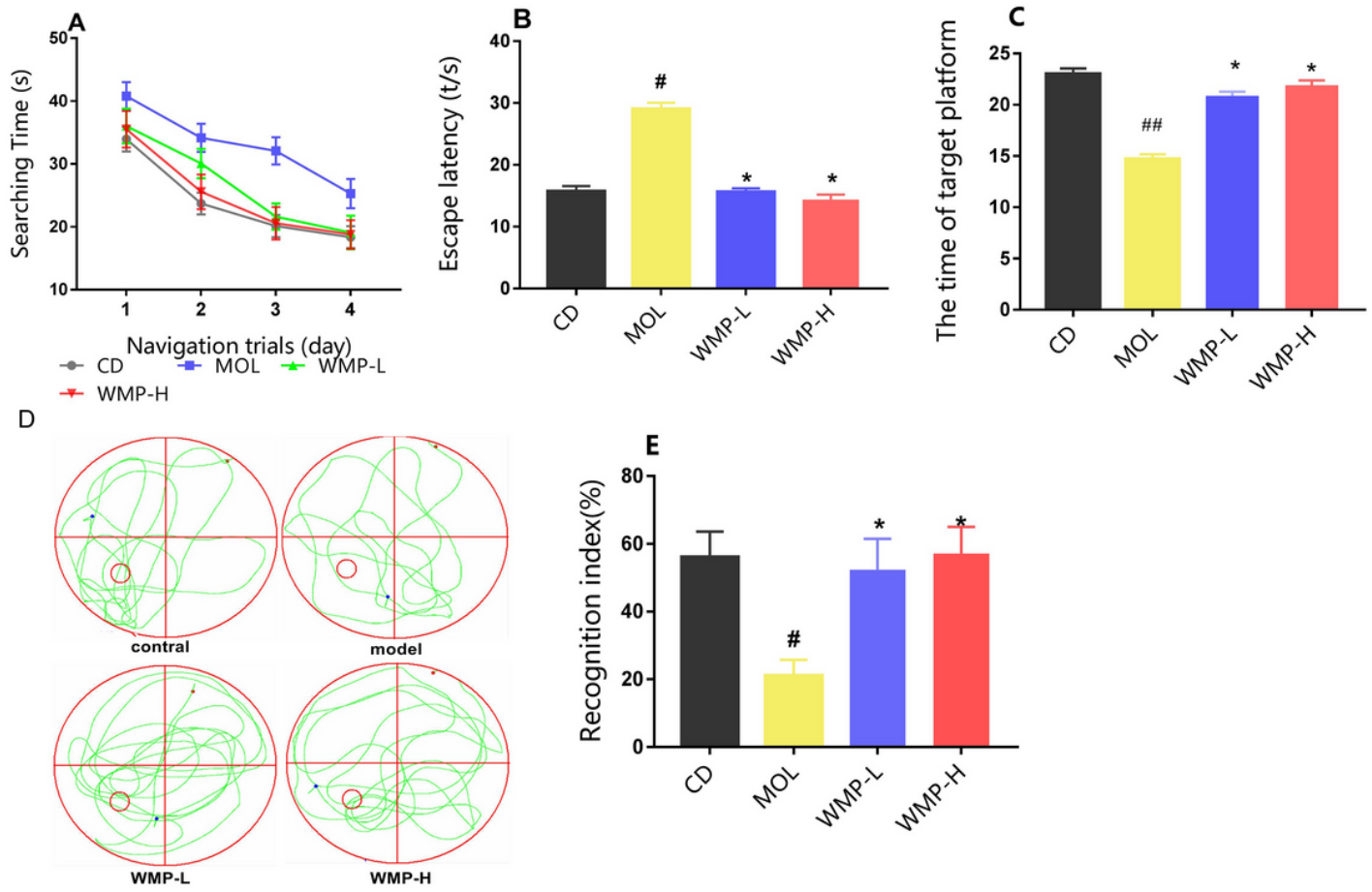

Figure 1

Behavioral test of WMP (800 and 1600 mg/kg/d) for improving the memory ability of AD mice induced by D-galactose. (A) The escape latency time in the first 4 days. (B-C) On the fifth day, the escape latency of exploration training and the stay time in the target quadrant. (D) On the fifth day, the Morris water maze trajectories of mice. (E) Recognition Index (DI) of mice in new object recognition experiment. Columns indicated mean ± SEM. Differences were expressed by ANOVA and denoted as follows: #p < 0.05, ##p < 0.01 vs. CD group; ∗p < 0.05 vs. MOL group.

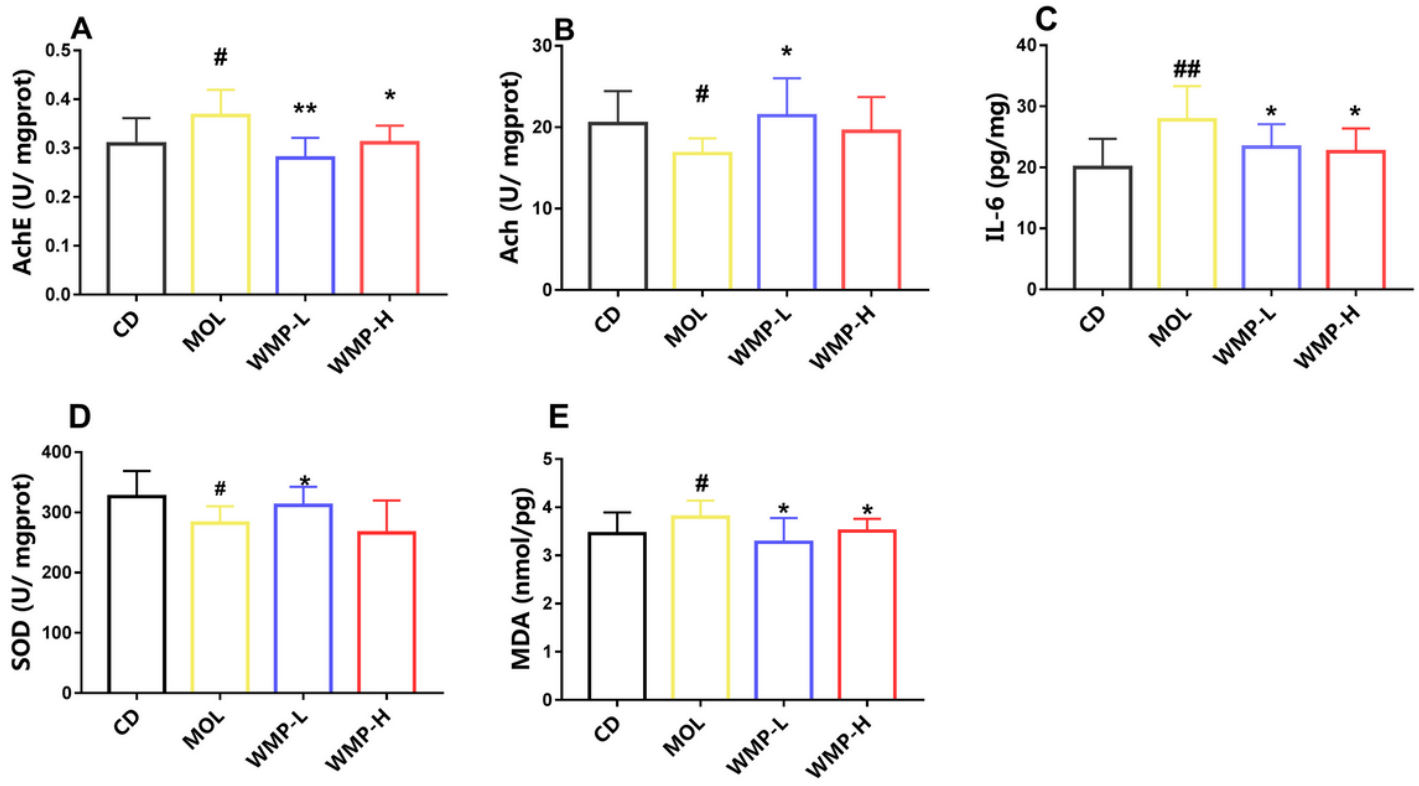

Figure 2

The effects of WMP (800 and 1600 mg/kg/d) on (A) the acetylcholinesterase activity (AchE), (B) acetylcholine level (Ach), (C) IL-6 level, (D) the activity of SOD, (E) the MDA level of MOL mice. Columns indicated mean ± SD (n = 9). Differences were expressed by ANOVA and denoted as follows: #p < 0.05, ##p < 0.01 vs. CD group; ∗p < 0.05, ∗∗p < 0.01 vs. MOL group.

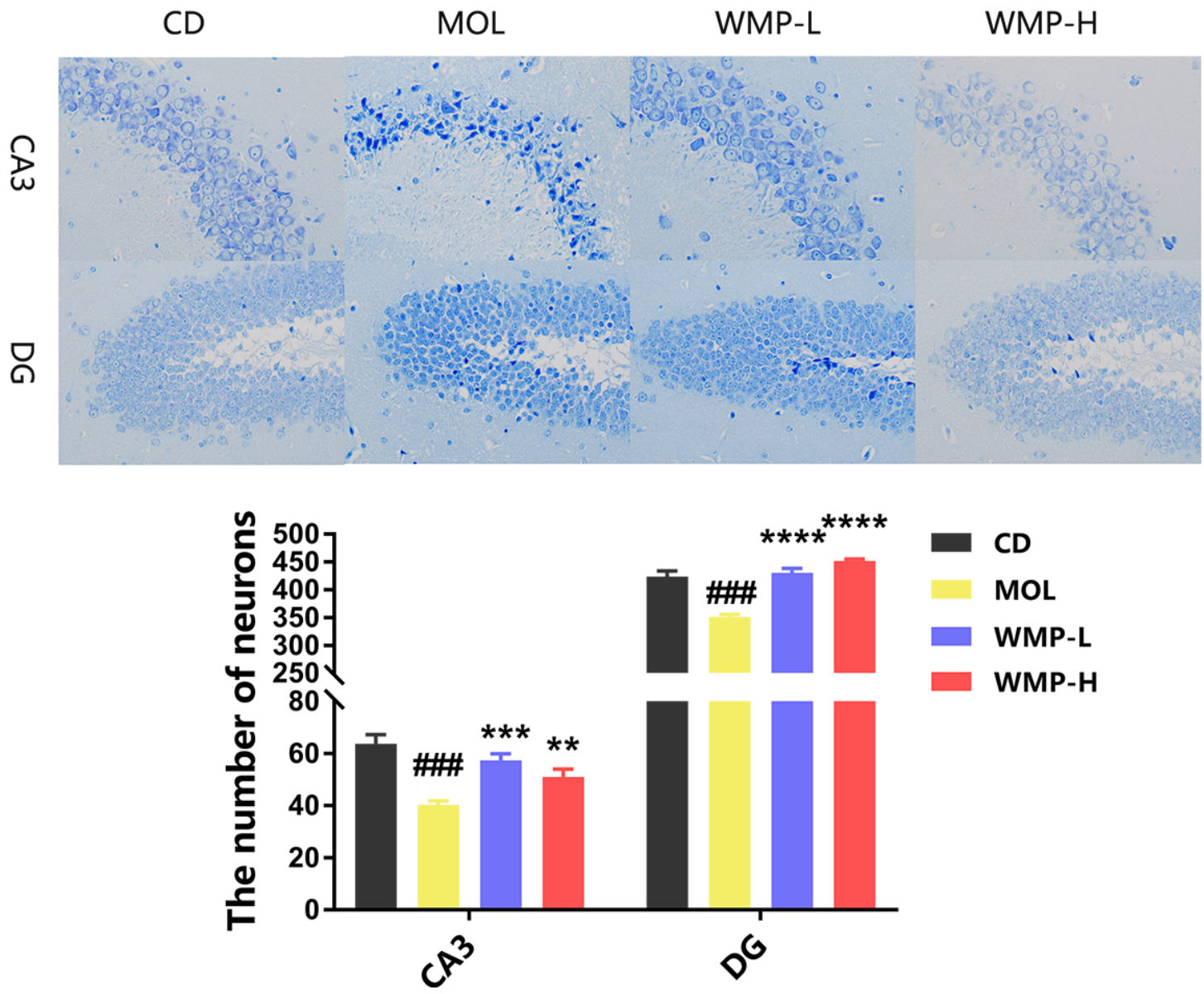

Figure 3

Nissl staining sections of the hippocampus (CA3, DG) in experimental mice (original magnification, 400 ×) and the numbers of neurons in hippocampus (CA3, DG) of experimental mice. Columns indicated mean ± SD (n = 3). Differences were carried out by ANOVA and denoted as follows: #p < 0.05, ##p < 0.01, ###p < 0.001 vs. CD group; ∗ p < 0.05, ∗∗p < 0.01 vs. MOL group.

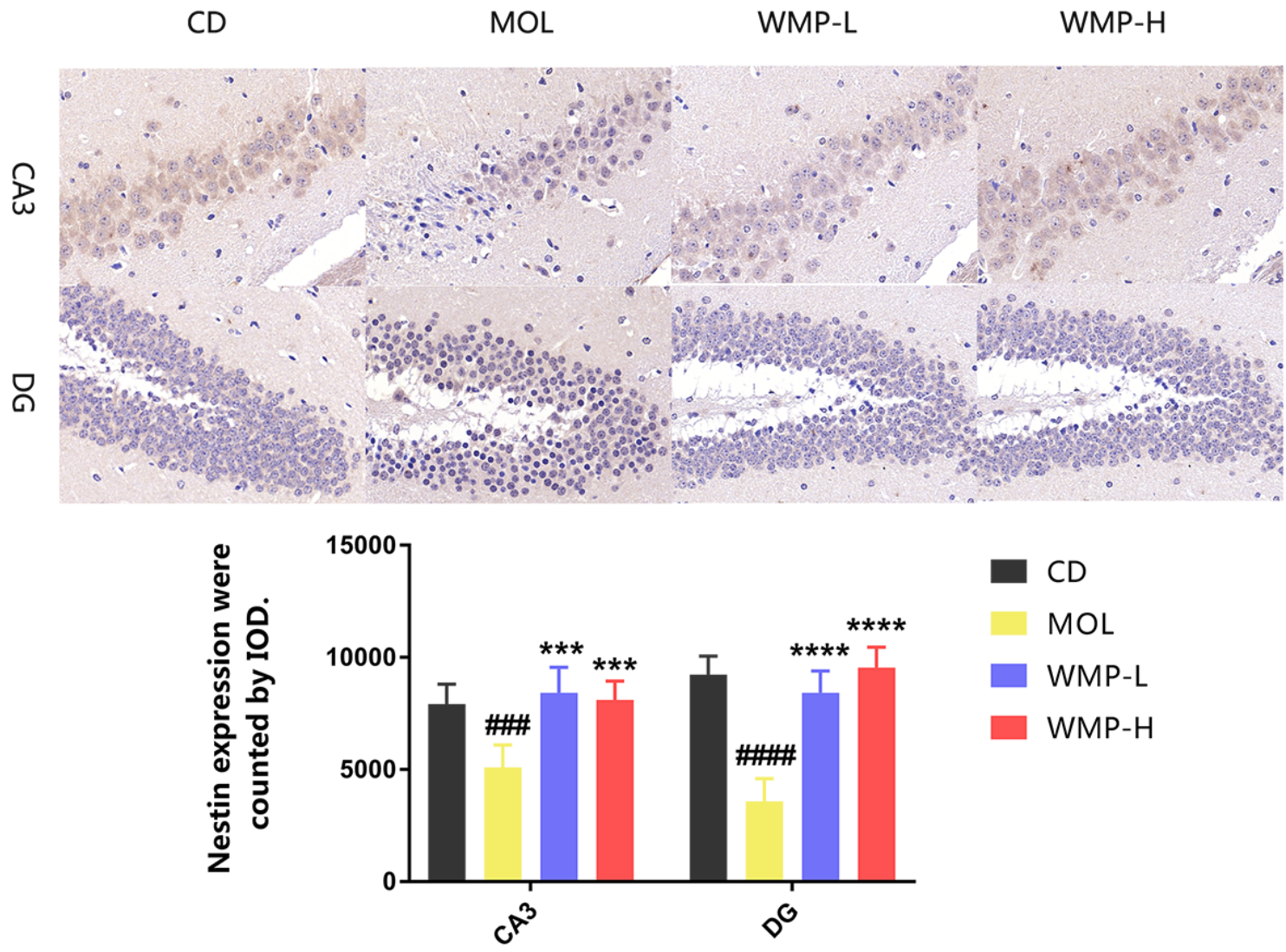

Figure 4

The Nestin expression of neural stem cells in the hippocampus (CA3, DG) of mice, image (up) and histogram (below) counted by IOD. Columns indicated mean ± SD (n = 3). Differences were carried out by ANOVA and denoted as follows: # $p < 0.05$, ## $p < 0.01$, ###$p < 0.001$, ####$p < 0.0001$ vs. CD group. ∗$p < 0.05$, ∗∗$p < 0.01$ vs. MOL group.

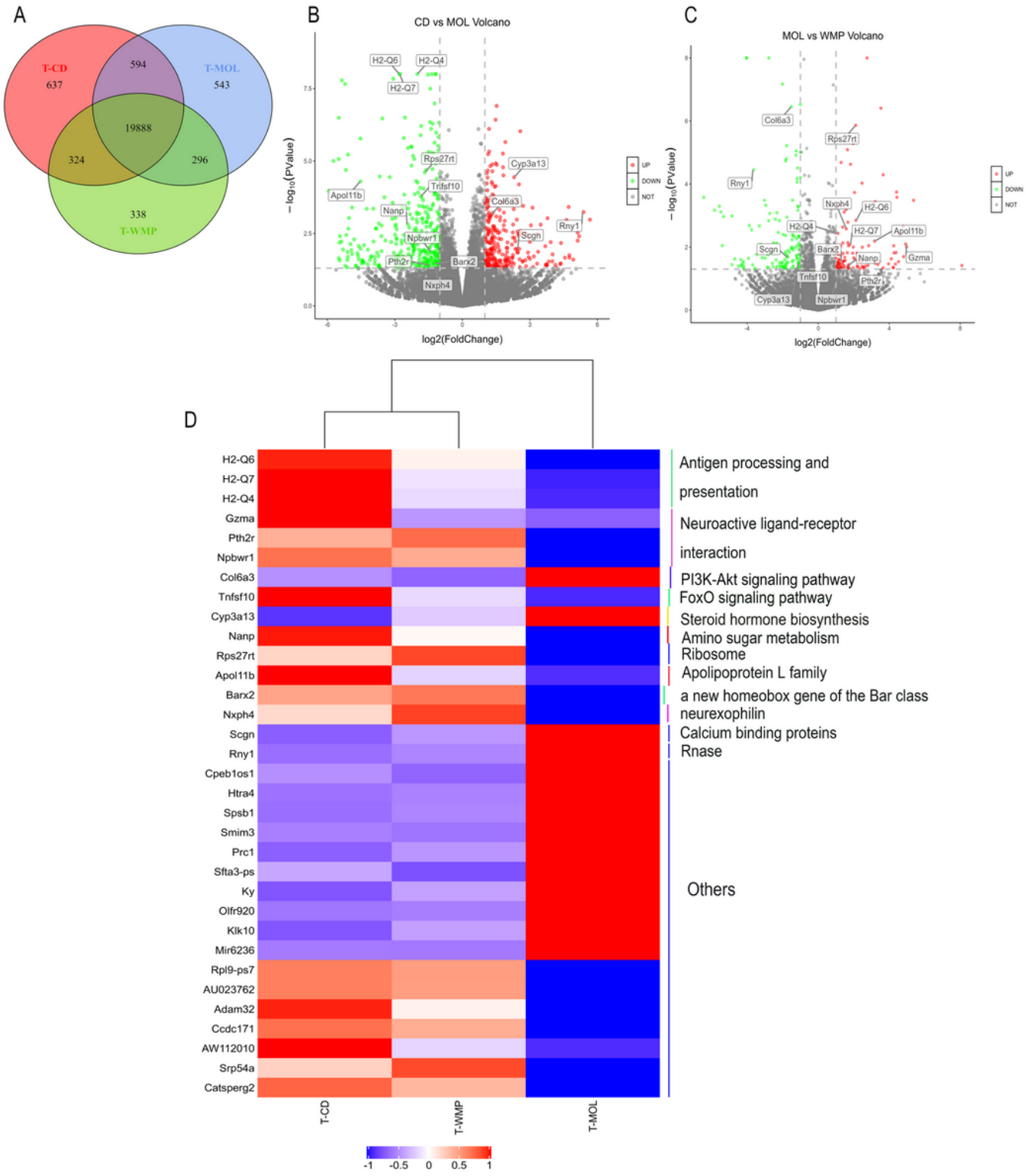

Figure 5

(A) Venn diagram displaying the differentially expressed genes in the hippocampus of CD, MOL, and WMP groups. (B) volcano plot displaying the differentially expressed genes between CD and MOL groups. (C) volcano plot displaying the differentially expressed genes between the WMP and MOL groups. (D) Euclidean distance by hierarchical algorithm displaying the differentially expressed genes of CD, MOL, and WMP groups.

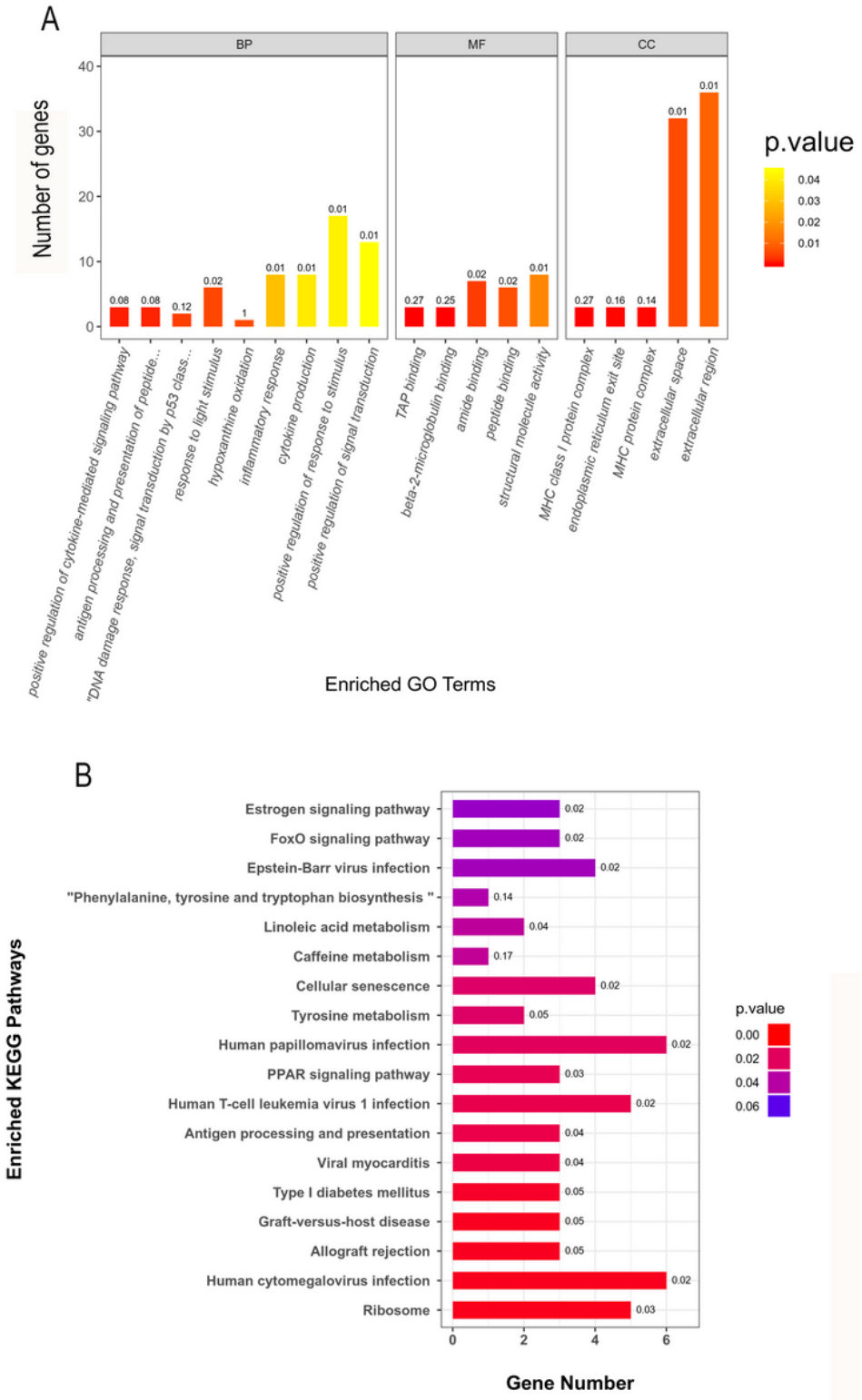

Figure 6

(A) GO analyses and (B) KEGG enrichment of the differentially expressed genes regulated by WMP in the hippocampus.

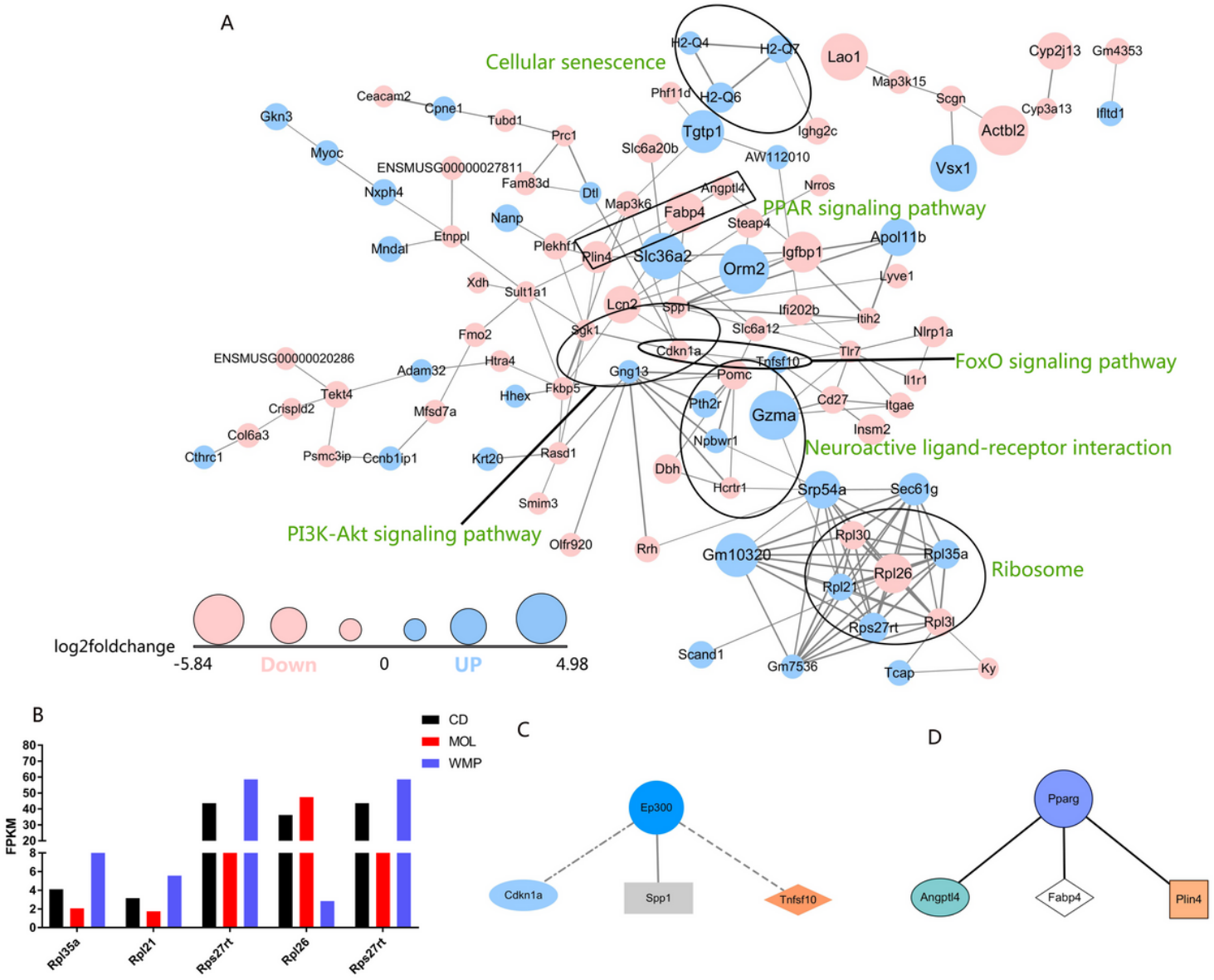

Figure 7

(A) PPI analysis of differentially expressed genes regulated by WMP in the hippocampus using STRING database and mapped by Cytoscape 3.6.0. (B) The FPKM level of Ribosomal family genes (Rpl35a, Rps27rt, Rpl3l, Rpl21, Rpl26). (C) Upstream transcription factor Ep300 regulated the process of Cdkn1a, Spp1, Tnfsf10. (D) Upstream transcription factor Pparg regulated the process of Angptl4, Fabp4, Plin4.